

Folate deficiency in normal human fibroblasts leads to altered expression of genes primarily linked to cell signaling, the cytoskeleton and extracellular matrix

Karen S. Katula^{a,*}, Alexandra N. Heinloth^b, Richard S. Paules^b

^aDepartment of Biology, University of North Carolina at Greensboro, Greensboro, NC 27402, USA

^bGrowth Control and Cancer Group, National Institute of Environmental Health Sciences, Research Triangle Park, NC 27709, USA

Received 18 May 2006; received in revised form 6 November 2006; accepted 22 November 2006

Abstract

The molecular basis linking folate deficiency to certain health conditions and developmental defects is not fully understood. We examined the consequences of folate deficiency on global gene expression by microarray and compared transcript levels in normal human fibroblast cells (GM03349) grown in folate-deficient and -sufficient medium. The largest represented groups from the selected genes functioned in cell signaling, the cytoskeleton and the extracellular matrix and included the Wnt pathway genes *DKK1*, *WISPI* and *WNT5A*. Twelve selected genes were further validated by qRT-PCR. Analysis of six genes at 4, 7, 10 and 14 days indicated that the relative differences in transcript levels between folate-sufficient and -deficient cells increases with time. Transcripts for 7 of the 12 selected genes were detected in the human lymphoblast cell line GM02257, and of these, changes in 4 genes corresponded to the results with fibroblast cells. Fibroblast cells were treated with the compounds homocysteine, methotrexate and the MEK1/2 inhibitor U0126, and relative transcript levels of six genes were determined. U0126 caused changes that more closely mimicked those detected in folate-deficient cells. The response of the *DKK1* and *TAGLN* gene promoters to folate deficiency and compounds was examined in NIH3T3 cells using luciferase reporter plasmids. Promoter activity for both genes was decreased by folate deficiency and methotrexate and unaffected by homocysteine. U0126 caused a decrease in *DKK1* promoter activity at 50 μ M and had no effect on *TAGLN* promoter activity. These findings suggest an alternative mechanism for how folate deficiency leads to changes in gene expression and altered cell function.

© 2007 Elsevier Inc. All rights reserved.

Keywords: *DKK1*; *WNT5A*; Lymphoblast; Fibroblasts; Homocysteine; Methotrexate

1. Introduction

Folates are essential water-soluble B vitamins that function as coenzymes primarily in reactions for the biosynthesis of certain nucleotides and methionine (Fig. 1). Significantly, folate deficiency is associated with numerous health problems including cardiovascular diseases [2–4], neurodegenerative disorders [5–7], cancer [8,9] and developmental defects such as neural tube defects [10–12], cleft palate [13,14] and heart defects [15,16]. The molecular basis linking folate deficiency to these health conditions remains incomplete and is likely to be complex due to the broad

biochemical and molecular consequences of folate deficiency as related to the folate pathway (Fig. 1).

Reduced nucleotide precursor pools and increased homocysteine, along with a reduction in the major methyl donor, *S*-adenosylmethionine (SAM), arise from folate deficiency. These biochemical changes have been associated with increased genomic instability [17–19], reduced DNA repair [20] and altered protein and DNA methylation [21–23], all of which have been proposed as mechanisms that link folate deficiency to various health effects, particularly cancer [8,24]. One potentially important consequence of folate deficiency that has not been thoroughly examined is changes in gene expression. These changes could occur by multiple pathways depending on the extent of the deficiency. Cells subjected to severe folate deficiency are more likely to accumulate DNA damage and respond by expressing DNA damage checkpoint, DNA repair and

* Corresponding author. Department of Biology, UNC Greensboro, Greensboro, NC 27404-6174, USA. Tel.: +1 336 334 4951; fax: +1 336 334 5839.

E-mail address: kskatula@uncg.edu (K.S. Katula).

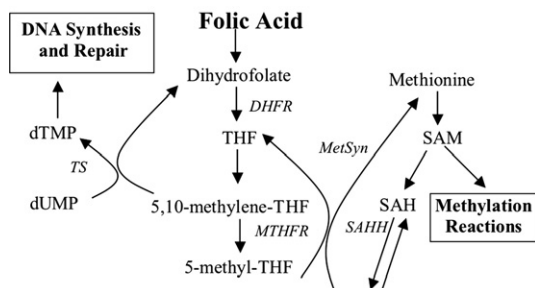


Fig. 1. Involvement of folate in pyrimidine biosynthesis and the homocysteine remethylation cycle. Based on a diagram in the study of James et al. [1]. Abbreviations include DHFR (for dihydrofolate reductase), MetSyn (for vitamin-B₁₂-dependent methionine synthase), MTHFR (for methylenetetrahydrofolate reductase), SAH (for *S*-adenosylhomocysteine), SAHH (for *S*-adenosylhomocysteine hydrolase), SAM (for *S*-adenosylmethionine), THF (for tetrahydrofolate) and TS (for thymidylate synthase).

apoptotic genes. Alterations in the expression of *p53* and *p21* have been associated with double strand breaks in folate-deficient cells [25]. Changes in gene expression may also result from altered gene-specific DNA methylation patterns as a consequence of reduced SAM. There are, however, only a few studies that provide evidence for such a link. These include the cancer-associated genes *p53*, *c-myc*, *c-fos*, *c-Ha-ras* and *p16INK4* [26–28] and the Alzheimer's genes *PS1* and *BACE* [29].

Much less is known regarding the consequences of folate deficiency on global gene expression. Considering the critical contributions of the folate pathway to cell function, particularly cell division, it might be expected that numerous alterations in gene expression would accompany fluctuations in the folate pathway and folate levels, possibly as a homeostatic response. To date, three studies that examine gene expression changes in folate-deficient cells by microarray have been published. Jhaveri et al. [30] detected only eight genes that responded to folate deficiency using a relatively small 2008 gene array and a transformed cell that was relatively insensitive to folate deficiency. None of these genes were related to DNA repair; instead, they were associated with cell adhesion and the cytoskeleton. Crott et al. [31] compared gene expression in the colonic mucosa of young and old rats via microarray. Folate-related genes were not altered, whereas genes associated with the extracellular matrix and cell attachment were. In contrast, Courtemanche et al. [32] found base and nucleotide excision repair genes and folate-related genes to be activated in lymphoblasts grown for 10 days in folate-deficient medium. Additional evidence that folate deficiency may alter the expression of genes that are not directly associated with DNA replication and damage is the finding that expression of the cell-signaling genes *Pax-3*, *Shh* and *En-2* is altered in mouse embryos, homozygous null for a folic acid binding protein transport protein [33].

To further understand the global consequences of folate deficiency, we compared gene expression in normal human fibroblast cells that were grown in folate-sufficient and -deficient medium via microarray analysis. We also

explored possible pathways that lead from folate depletion to the changes in transcript levels.

2. Materials and methods

2.1. Cell cultures and conditions

GM03349 are normal human dermal fibroblasts obtained from the National Institute of General Medical Sciences (NIGMS) Human Genetic Mutant Cell Repository (Corriell, Camden, NJ). The cells were derived from a 10-year-old male. For routine culture, GM03349 cells were grown at 37°C in a humidified 95% air/5% CO₂ atmosphere in Minimum Essential Medium (MEM) supplemented with 10% fetal bovine serum (FBS; Invitrogen, Carlsbad, CA) and 2 mM L-glutamine (referred to as MEM-C). For studies involving folate deficiency, custom-made MEM was prepared at the National Institute of Environmental Health Sciences (NIEHS), with and without folic acid, which was supplemented with dialyzed FBS (Invitrogen) and L-glutamine. These media were referred to as FS-dMEM-C and FD-dMEM-C for folate-sufficient and folate-deficient custom-made MEM containing dialyzed FBS, respectively. FS-dMEM-C and FD-dMEM-C were identical, except for the lack of folic acid in FD-dMEM-C. Cells were initially expanded in MEM-C, collected and plated in T-175 flasks containing FS- or FD-dMEM-C at 5.4×10^5 cells per flask for 3 or 4 days, depending on the nature of the experiment. The cells were then collected and replated in T-175 flasks, 100-mm plates (at 1.75×10^5 cells per plate) or 60-mm plates (at 6.5×10^4 cells per plate) in FS-dMEM-C or FD-dMEM-C. For periods of folate deficiency longer than 7 days, cells (FS and FD) were collected and replated at the given cell numbers and grown no longer than 3 or 4 days. GM03349 cells used for microarray analysis were grown in FS- and FD-dMEM-C in T-175 flasks for 4 days, collected and replated in 50×100 mm dishes and cultured for another 3 days. Two biological replicas were generated for microarray analysis (Sets 1 and 2). The GM02254 cell line consists of EBV-transformed human lymphoblasts obtained from NIGMS. The cells were grown as a suspension culture in RPMI 1640 medium containing 15% FBS plus 2 mM L-glutamine. Custom-made RPMI 1640 was prepared at NIEHS, with and without folic acid, and complete medium was prepared using dialyzed FBS. The mouse fibroblast cell line NIH3T3 was obtained from the American Type Culture Collection and grown in Dulbecco Eagle's medium supplemented with 10% FBS, 3.7 g/L sodium bicarbonate, 3.57 g/L HEPES, 1.0% penicillin/streptomycin (10,000 IU/ml and 10,000 mg/ml) and 0.1% (v/v) Amphotericin B fungicide (250 µg/ml).

2.2. Flow cytometry

For analysis of cell cycle phases, cells were labeled with Brdu and propidium iodide [34]. Essentially, cells were incubated with 10 µM Brdu for 2 h, collected and fixed in 70% methanol. The fixed cells were permeabilized and

incubated with a primary mouse anti-BrdU antibody (Becton Dickinson, Franklin Lakes, NJ) and then with a donkey FITC-conjugated antimouse antibody (Jackson ImmunoResearch Laboratories, West Grove, PA). The cells were incubated with propidium iodide (5 $\mu\text{g}/\text{ml}$) prior to analysis on a Becton Dickinson FACSsort (San Jose, CA).

2.3. RNA preparation

GM03349 cells were collected from 100-mm dishes by scrapping into cold phosphate-buffered saline (PBS). Cells were collected by centrifugation, washed once in cold PBS and repelleted. GM02254 cells were collected from culture medium by centrifugation, washed one time in PBS and repelleted. Cell pellets were stored in liquid nitrogen. RNA was isolated from the cell pellets using a Qiagen RNeasy Midi or Mini Kit (Qiagen, Inc., Valencia, CA) according to the instructions of the manufacturer. RNA quality was assessed using an Agilent BioAnalyzer (Santa Clara, CA).

2.4. Microarray analysis

cDNA synthesis, chip hybridization and data analysis were conducted as essentially described [35,36] with the

following modifications and details. Twenty-five micrograms of total RNA was used for cDNA synthesis and incorporation of Cy3-dUTP or Cy5-dUTP. Each control and treated sample pair was hybridized in quadruplicate with the treated sample labeled twice with Cy3 and then twice with Cy5 (fluor reversal). The microarray used in this study was the NIEHS Human Oligo chip containing approximately 17,000 70-mer oligonucleotides from the Operon Human Oligo Set V1.1. The gene list can be found at <http://dir.niehs.nih.gov/microarray/inhousearrays.htm>. Fluorescent intensities were measured with an Agilent DNA Microarray scanner (Palo Alto, CA). The signal intensities were quantified and normalized from the spots on the image files utilizing IPLabs image-processing software (Scanalytics, Inc., Fairfax, VA) with the Array Suite 2.0 extension (National Human Genome Research Institute, Bethesda, MD) [37]. Those genes differentially expressed at the 95% confidence level in both hybridizations per RNA pair (folate-sufficient and folate-deficient cells) were initially selected from each set. At this level, the probability of detecting a gene as differentially expressed by chance is $P < .0025$. To assure reproducibility of the observed changes

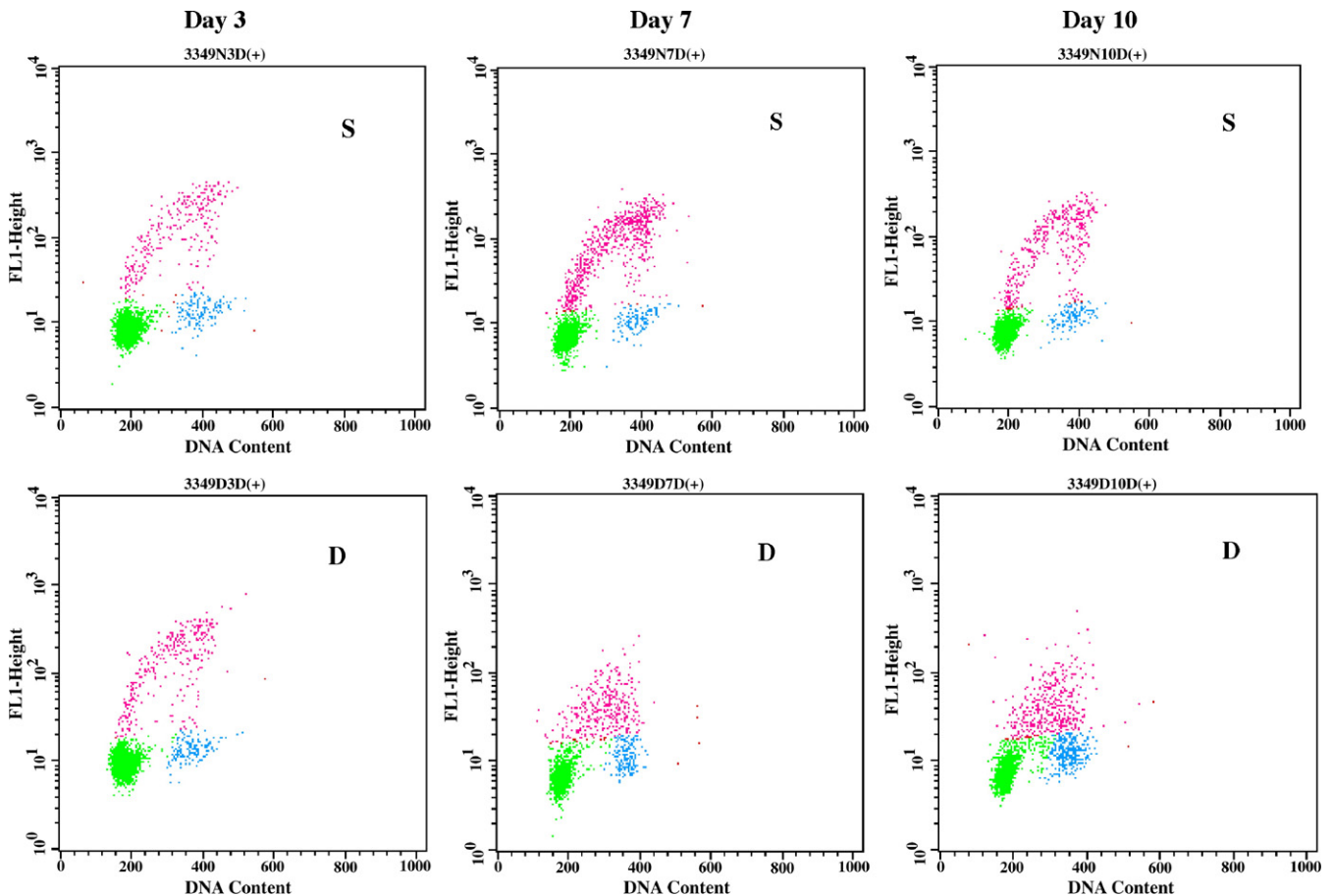


Fig. 2. Cell cycle phase distribution in folate-sufficient (S) and -deficient (D) cells. Cells were grown in folate-sufficient (S) and -deficient (D) medium for 3, 7 and 10 days. BrdU was added to the medium 2 h prior to cell collection. Collected cells were stained for incorporated BrdU (FITC) and DNA (propidium iodide or PI) as described in Section 2 and analyzed by flow cytometry. DNA content is indicated by relative fluorescence from PI on the x-axis, and incorporated BrdU is indicated by relative fluorescence from FITC on the y-axis. Cells colored red in the diagram are labeled with both PI and FITC, representing S-phase cells.

Table 1
Selected sequences from cluster analysis

Accession no.	Symbol	Gene description	Fold change (Set 1/Set 2)
Cell-cell communication			
L20861*	<i>WNT5A</i>	Wingless-type MMTV integration site family member	3.08/1.71
U61412	<i>PTK6</i>	Protein tyrosine kinase 6	2.13/1.42
D83492*	<i>EPHB6</i>	Ephrin receptor, EphB6	2.53/2.28
NM_000885	<i>ITGA4</i>	Integrin, alpha 4	2.00/1.67
NM_001449	<i>FHL1</i>	Four and a half LIM domains 1	2.04/1.70
AF100779*	<i>WISP1</i>	WNT1 inducible signaling pathway protein 1	1.99/1.97
U67784	<i>CMKOR1</i>	Chemokine orphan receptor 1	1.87/1.57
AJ002030	<i>PGRMC2</i>	Progesterone receptor membrane component 2	1.81/1.71
AF110640	<i>CCRL1</i>	Chemokine (C-C motif) receptor-like 1	1.74/1.90
AF242769	<i>LOC51334</i>	Mesenchymal stem cell protein DSC54	1.67/1.53
U90920	<i>PARG1</i>	PTPL1-associated RhoGAP1	1.62/1.34
AL137332	<i>DRCTNNB1A</i>	Down-regulated by Ctnnb1, a	1.50/1.31
L27560	<i>IGFBP5</i>	Insulin-like growth factor binding protein 5	1.40/2.80
M90657	<i>TMSF1</i>	Transmembrane 4 superfamily member 4	0.98/0.62
AF334184*	<i>FKSG42</i>	Contains RhoGAP domain	0.59/0.55
NM_012242*	<i>DKK1</i>	Dickkopf homolog 1	0.32/0.30
Cytoskeleton			
D25248	<i>AFAP</i>	Actin filament associated protein	2.6/1.96
J05582	<i>MUC1</i>	Mucin 1, transmembrane	1.58/1.94
X13839	<i>ACTA2</i>	Actin, alpha 2, smooth muscle, aorta	0.83/0.73
Y09836	<i>MAP1B</i>	Microtubule-associated protein 1B	0.78/0.64
AF234532	<i>MYO10</i>	Myosin X	0.63/0.53
M95787*	<i>TAGLN</i>	Transgelin, actin crossing linking	0.61/0.72
J00073	<i>ACTC</i>	Actin, cardiac	0.32/0.15
Extracellular matrix			
AL137540*	<i>NTN4</i>	Netrin 4	1.80/2.39
AK000953		Weakly similar to Sus scrofa decorin mRNA	1.79/2.22
D50406	<i>RECK</i>	Reversion-inducing, cysteine-rich protein with kazal motifs	1.76/1.29
X05232	<i>MMP3</i>	Matrix metalloproteinase 3	0.86/0.50
NM_013363	<i>PCOLCE2</i>	Procollagen C-endopeptidase enhancer 2	0.77/0.60
Membrane proteins/transporters			
NM_000165*	<i>GJA1</i>	Gap junction protein, alpha 1, 43 kDa (connexin 43)	2.14/1.44
NM_007289	<i>MME</i>	Membrane metallo-endopeptidase	1.79/1.25
U17077*	<i>BENE</i>	BENE protein, raft protein, associates with caveolin-1	1.02/0.50
U97519*	<i>PODXL</i>	Podocalyxin-like	0.73/0.52
Transcription			
AB015427	<i>ZNF219</i>	Zinc finger protein 219	2.66/1.60
U89337	<i>CREBL1</i>	cAMP responsive element binding protein-like 1	1.67/1.86
X64229*	<i>DEK</i>	DEK oncogene (DNA binding)	1.48/1.51
S78825	<i>IDI</i>	Inhibitor of DNA binding 1	0.96/0.47
Apoptosis			
AF002697*	<i>BNIP3</i>	BCL2/adenovirus E1B 19 kDa interacting protein 3	2.00/1.98
AL132665	<i>BNIP3L</i>	BCL2/adenovirus E1B 19 kDa interacting protein 3-like	1.92/1.68
Cell cycle			
L13720	<i>L13720</i>	Growth arrest-specific 6	1.37/1.46
D79988	<i>KNTC1</i>	Kinetochore associated 1	1.31/1.60
Stress			
L19686	<i>MIF</i>	Macrophage migration inhibitory factor	1.70/1.63
AJ243191	<i>HSPB7</i>	Heat shock 27 Da protein family, member 7	0.70/0.46
Nucleic acid metabolism			
S81916	<i>PGK1</i>	Phosphoglycerate kinase 1	1.61/1.55
X02308	<i>TYMS</i>	Thymidylate synthetase	1.59/1.63
X60673	<i>AK3</i>	Adenylate kinase	1.52/1.83
Other metabolism			
AF131821	<i>MGLL</i>	Monoglyceride lipase	1.60/1.70
NM_024307	<i>MGC4171</i>	Hypothetical protein MGC4171	1.56/1.73
U18932	<i>NDST1</i>	N-deacetylase/N-sulfotransferase	1.36/1.55
Immune			
X87212	<i>CTSC</i>	Cathepsin C	1.50/1.51
AJ275439		Immunoglobulin heavy-chain V region	0.58/0.62
Exocystosis/Endocystosis			
AB016811	<i>ARL7</i>	ADP-ribosylation factor-like 7	3.26/1.90

Table 1 (continued)

Accession no.	Symbol	Gene description	Fold change (Set 1/Set 2)
M38591	<i>S100A10</i>	S100 calcium-binding protein A10	2.08/1.54
Oncogene M13211		Human translocated c-myc oncogene (Ly65) in mu switch region of the IgG heavy-chain locus	2.08/1.54
Protein turnover AB037771	<i>USP53</i>	Ubiquitin-specific protease 53	2.81/1.81
Unknown AL139188		Human DNA sequence from clone RP11-90M5	2.64/1.96
U30521	<i>C5orf13</i>	Chromosome 5 open-reading frame 13, P311	2.55/1.95
AL079279		<i>Homo sapiens</i> mRNA full-length insert cDNA clone EUROIMAGE 248114	2.08/1.56
NM_016206	<i>FLJ38507</i>	Colon-carcinoma-related protein	1.93/1.82
AL049798		Human DNA sequence from clone RP4-797M17	1.33/1.79
AL031659		Human DNA sequence from clone RP1-150O5	0.70/0.80
AL021154		Human DNA sequence from clone RP1-150O5	0.44/0.37

Genes are listed in descending order according to Set 1 fold-change values. Those in boldface show a decrease.

between technical replicates, only genes that were detected in three out of four hybridizations were included in further analysis. Therefore, selecting differentially expressed genes expressed at the 95% confidence level ($P = .05$) for three out of the four technical replicates has a probability of .00000396. Also, the coefficient of variation (CV) for each gene across replicate hybridizations was calculated, using the \log_2 ratio intensity values of the genes detected as differentially expressed at a given confidence level. Genes with a CV value greater than 0.8 were eliminated from further statistical analysis. The biological replicates (Sets 1 and 2) were compared by cluster analysis, and shared genes were identified. In addition, a comparison between Sets 1 and 2 was carried out to identify genes that changed in the same direction but was at 95% confidence for only one of the two sets. The microarray data GEO accession number is GSE3548.

2.5. Quantitative real-time PCR

Quantitative real-time (qRT)-PCR was conducted for specific gene sequences using Assay-on-Demand gene specific primers (Applied Biosystems, Foster City, CA). We converted 2.5 μg of total RNA to cDNA as described in the study of Heinloth et al. [35]. This cDNA was diluted 1:20 in water and amplified using the TaqMan Universal PCR Master Mix (Applied Biosystems) and gene-specific 20 \times Assays-on-Demand gene expression mix. Five replicates were conducted for each gene-specific primer. The amplification reactions were conducted on an ABI Prism 7900HT Sequence Detector (Applied Biosystems) using the following cycling conditions: initially, 50 $^\circ\text{C}$ for 2 min and 95 $^\circ\text{C}$ for 10 min, followed by 40 cycles of 95 $^\circ\text{C}$ for 15 s and 60 $^\circ\text{C}$ for 1 min. The cycling data were analyzed using Sequence Detection System version 2.1 software (Applied Biosystems). Glyceraldehyde 3-phosphate dehydrogenase (*GAPDH*) sequences were amplified in each sample. Gene-specific sequence levels were normalized with the value for *GAPDH*.

2.6. Construction of the *DKK1* and *TAGLN* luciferase reporter constructs and stable cell lines

The *DKK1* and *TAGLN* upstream sequence regions were obtained from the UC-Santa Cruz Genome Browser (<http://genome.ucsc.edu>) using the accession numbers NM_012242 and M95787. Primers were synthesized and used to amplify an approximately 1000-bp region including 5'-UTR and the beginning of the cDNA sequences for each gene. *Bgl*II sites were included on the primers for cloning into the luciferase vector, pGL2-Basic (Promega, Madison, WI). The resulting clones were confirmed by DNA sequencing. For generating stable cell lines in NIH3T3, the plasmids were precipitated in a molar ratio of 5:1 with the selection vector pMC1neo polyA (Stratagene, La Jolla, CA). Approximately 10 μg of total plasmid DNA was transfected per 100-mm plate containing 2×10^5 NIH3T3 cells by the calcium phosphate method using the Profection kit (Promega). Two days later, the medium was changed and 500 $\mu\text{g}/\text{ml}$ of G418 (Sigma-Aldrich, St. Louis, MO) was added. The medium was changed every 2 or 3 days until complete cell death occurred. The resistant cells were collected as a group and expanded. Cells were collected and stored in liquid nitrogen.

2.7. Treatment of cells with methotrexate, homocysteine and U0129

GM03349 cells were plated in 100-mm plates at 2.5×10^5 cells per plate the day prior to treatment. The NIH3T3 cells that were stably transfected with the *DKK1* and *TAGLN* luciferase reporter vectors were plated in 24-well dishes at 2×10^4 cells per well. Compounds were prepared fresh. A vial of U0126 (Sigma-Aldrich) was dissolved in dimethyl sulfoxide (DMSO) to generate a 10-mM stock. Equal amounts of DMSO were added to the untreated dish to serve as the control for the U0126-treated cells. A 300- or 600- μM stock of methotrexate (Sigma-Aldrich) was prepared in water and brought into solution with addition of 5 N

NaOH. Homocysteine (Sigma-Aldrich) was prepared as a 10-mM stock in water and adjusted to pH 7.0 with 5 N NaOH. All stocks were filter sterilized prior to addition. Cells were incubated for 24 h after addition of compounds. The cells were collected for isolation of RNA as previously described or collected as cell lysates for luciferase assays.

2.8. Luciferase assays

Cells were washed with PBS and 100 to 150 μ l of 1 \times Cell Lysis Buffer (Promega) added per well. The cells were incubated at 37°C for 15 min, and the lysates were collected and stored at –20°C. We assayed 30 or 40 μ l of cell lysate in a Berthold (Oak Ridge, TN) LUMAT LB9501 luminometer to obtain values of relative light units. Protein concentration of the lysate was determined using a protein assay kit (Bio-Rad Laboratories, Melville, NY). The level of luciferase activity was expressed as relative light units per microgram of protein.

2.9. Measurements of intracellular folate levels

Levels of intracellular folate were determined using the *L. casei* microbiological assay [38]. Cells grown under folate-deficient and -sufficient culture conditions for microarray analysis were collected by centrifugation. The cell pellets were analyzed for folate levels as described.

3. Results

3.1. Comparison of gene expression in cells grown in folate-sufficient and -deficient medium

We chose a decrease in population growth rate and DNA synthesis as indicators of folate deficiency in the normal cultured dermal human fibroblasts GM03349 used in this study. Our intent was to analyze cells that are not acutely depleted of folate, as such cells would be more likely to express genes that are primarily related to apoptosis or necrosis. The fibroblast cells were grown in folate-deficient and -sufficient medium for 3, 7 and 10 days, and population growth rates and cell cycle phase distribution were determined. At Day 3, folate-sufficient and -deficient cells appeared similar based on these parameters (data not shown and Fig. 2). At Days 7 and 10, folate-deficient cells showed a decrease in population growth rate (data not shown) and rate of DNA synthesis, as indicated by a reduction in Brdu incorporation in the S-phase cells of the folate-deficient cells relative to the folate-sufficient cells [Fig. 2, compare sufficient (S) to deficient (D) panels of Days 7 and 10]. Based on these data, Day 7 was chosen for array analysis.

Cells were grown in folate-sufficient and -deficient medium for 7 days. To maintain similar cell densities, we collected and replated cells in folate-sufficient and -deficient medium at identical densities 3 days prior to collection at Day 7. At the time of collection, the cells were subconfluent in both groups. RNA was isolated from these cells and used in array analysis. Two biological replicas (Sets 1 and 2)

were generated and analyzed independently. Analysis of the intracellular folate levels indicated that the folate levels in Sets 1 and 2 were reduced in folate-deficient and -sufficient cells to 1.3% and 0.7%, respectively.

Differentially regulated genes were selected based upon a 95% confidence level cutoff in relation to fold change and showed the same direction of change on three out of the four chips. For Sets 1 and 2, 64 and 75 genes were identified, respectively. These gene lists were compared by hierarchical cluster analysis, and the expression levels of these genes were compared with the same gene in the opposite set (data not shown). From this comparison, genes that displayed a similar direction of change in three of the four hybridizations were selected and were on the selected gene list (95% confidence level; $P = .05$) for one set or for both of the sets (1 or 2). These genes are listed in Table 1, along with their functional groupings and fold change in Sets 1 and 2.

3.2. qRT-PCR analysis

Twelve genes were selected from Table 1 for validation by qRT-PCR. These were chosen based on availability of primers, gene identity and direction of change. Fold change values from the array data and qRT-PCR were compared for Sets 1 and 2 (Fig. 3). Generally, all 12 genes displayed the same direction of change, comparing the microarray and qRT-PCR data, although the degree of change differed. *DEK* and *BENE* are two exceptions; no changes were detected for one of the four values.

3.3. Time course of gene expression changes

It would be expected that changes in transcript levels as detected by microarray and verified by qRT-PCR would display a pattern of change over time consistent with decreasing cellular folate, that is, less difference between

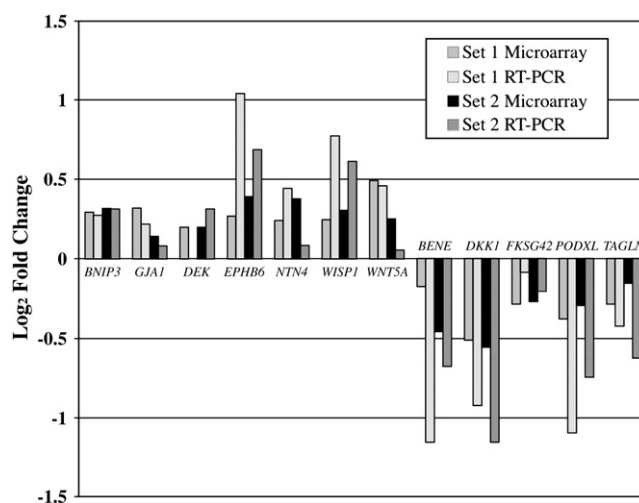


Fig. 3. qRT-PCR validation of a subset of genes. Gene-specific primers for each of the indicated genes were used in qRT-PCR with Set 1 and Set 2 microarray RNA samples. The log₂ fold change of the folate-deficient cells relative to the folate-sufficient cells is shown. Gene names for the abbreviations can be found in Table 1.

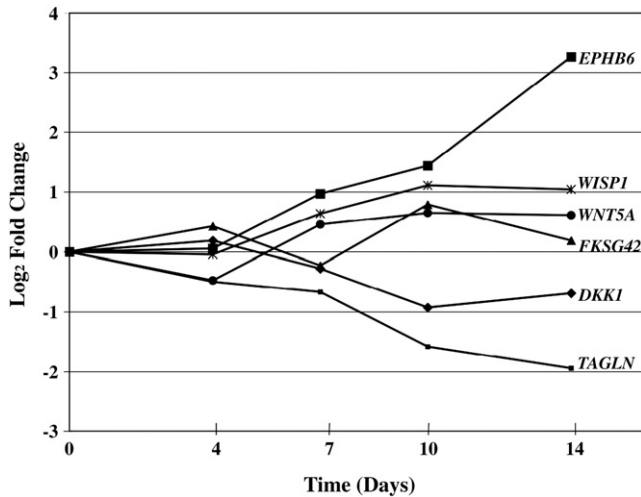


Fig. 4. Time course of transcript levels for selected genes. Normal human fibroblasts were grown in folate-sufficient and -deficient medium for 4, 7, 10 and 14 days. Relative transcript levels in RNA isolated from the cells for the genes indicated were determined by qRT-PCR. Gene names can be found in Table 1. The Day 0 value was set at zero.

folate-sufficient and -deficient cells at earlier time points and a greater difference with more time in folate-depleted medium. Normal human fibroblast cells were grown in folate-sufficient and -deficient medium for 4, 7, 10 and 14 days. RNA isolated from the cells was analyzed by qRT-PCR with primers for six of the genes shown in Fig. 3 (*DKK1*, *EPHB6*, *FKSG42*, *TAGLN*, *WISP1* and *WNT5A*). The data for one trial are shown in Fig. 4. A second trial, excluding Day 14 samples, gave similar results. At Day 4, gene transcript levels are more similar between the folate-sufficient and -deficient cells (closer to zero). The relative fold change increased with additional days in folate-depleted medium. One exception is *FKSG42*, which did not show a consistent pattern. Of the 12 selected genes, *FKSG42* was least affected by folate deficiency. The delay in response to folate deficiency is most likely due to the time required to deplete intracellular folates. Significantly, these data provide additional confirmation of a folate-deficiency effect on these genes and suggest that, at longer periods of folate deficiency, at least some of the same genes would have been selected by microarray analysis.

3.4. Effects of folate depletion on gene expression in human lymphoblast cells

The gene probes selected for gene validation in human fibroblast cells (see Fig. 3) were used to analyze changes in transcript levels in the human lymphoblast cell line GM02259. These data will indicate the extent to which these gene expression changes are specific to a particular cell type. Lymphocytes are known to be particularly sensitive to folate depletion, and the molecular consequences of folate deficiency have been investigated in these cells [18,19,39]. Lymphoblast cells were assayed at Day 4, as by Day 7, there was cell loss. As shown in Table 2, only 7 out of the 12 gene transcripts were detected in lymphoblast cells. Of these, four displayed the same direction of change to the human fibroblast cells (*GJAI*, *DEK*, *EPHB6* and *WNT5A*), and one was in the opposite direction (*FKSG42*). Relative fold change for the *BNIP3* transcript is only slightly decreased in lymphoblasts compared to an increase in fibroblasts, whereas the relative fold change in *PODXL* transcript levels is inconsistent in the lymphoblasts.

3.5. Comparison of gene expression in folate-deficient and methotrexate-, homocysteine- and U0126-treated human fibroblast cells

The six genes we chose for further analysis are not obviously linked to DNA damage or repair pathways. An alternative explanation for the observed changes in gene expression is increased homocysteine due to folate deficiency (see Fig. 1). To test this possibility, we determined the fold changes in transcript levels of *DKK1*, *EPHB6*, *FKSG42*, *TAGLN*, *WISP1* and *WNT5A* relative to untreated cells, using RNA isolated from human fibroblast cells treated with 50 μ M homocysteine for 24 h. Transcript levels were also compared in folate-deficient cells relative to folate-sufficient cells that were grown from the same cell passage, thus providing further confirmation of the microarray and RT-PCR data (shown in Fig. 3). As seen in Fig. 5, the relative change in transcript levels for the six genes in the homocysteine-treated cells did not correspond to the folate-deficient cells. Relative transcript levels were reduced (*EPHB6*, *WISP1* and *WNT5A*) and did not increase, as in

Table 2
Relative changes in transcript levels of selective genes in human lymphoblast and fibroblast cells

	<i>BNIP3</i>	<i>GJAI</i>	<i>DEK</i>	<i>EPHB6</i>	<i>FKSG42</i>	<i>PODXL</i>	<i>WNT5A</i>
Lymphoblasts	–	+	+	+	+	±	+
	0.79	6.44	1.44	14.51	5.62	0.68	4.36
	0.90	5.69	1.52	24.91	6.09	1.36	4.00
Fibroblasts	+	+	+	+	–	–	+
	1.99 (± 0.05)	1.58 (± 0.19)	1.55 (± 0.22)	5.04 (± 2.08)	0.68 (± 0.06)	0.30 (± 0.10)	1.95 (± 0.30)

Relative transcript levels were compared by qRT-PCR using RNA isolated from cells grown in folate-deficient and -sufficient medium for 4 days (GM02254, lymphoblasts) and 7 days (GM03349, fibroblasts). Minus (–) and plus (+) symbols represent a decrease or increase, respectively, in the relative gene transcript levels in the folate-deficient cells compared with the folate-sufficient cells. The $2^{-\Delta\Delta CT}$ (relative fold change) values from two independent trials of lymphoblasts are shown. The relative fold-change values for the fibroblasts represent the averages of four or seven determinations from Set 1 and Set 2 RT-PCR, microarray data and additional independent qRT-PCR assays, with standard error values enclosed in parentheses.

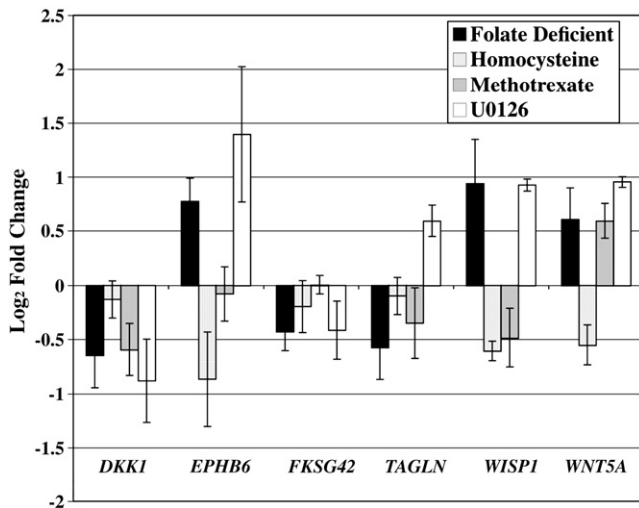


Fig. 5. Effects of methotrexate, homocysteine and the MEK1/2 inhibitor U0126 on transcript levels of selected genes. Normal human fibroblast cells (GM03349) were treated with 1 μ M methotrexate, 50 μ M homocysteine and 10 μ M U0126 for 24 h as described in Section 2. From the same cell passage, cells were grown for 7 days in folate-sufficient and -deficient medium. RNA was isolated from the cells and analyzed for transcript levels of the genes shown by qRT-PCR. Fold change for the treated cells is relative to the untreated cells, and for the folate-deficient cells, fold change is relative to cells grown in folate-sufficient medium. Error bars indicate \pm S.E.; $n=3$.

folate-deficient cells, or did not change (*DKK1*, *TAGLN* and *FKSG42*).

Decreased Ras signaling has been detected in folate-deficient cells [40]. Thus, we examined if any of the observed changes in gene expression are linked to the Ras pathway. Human fibroblast cells were treated with the MEK1/2 inhibitor U0126 for 24 h, and the relative fold change in transcript levels for the six selected genes was measured by qRT-PCR (Fig. 5). Of the six genes, all but *TAGLN* displayed the same direction of change as in the folate-deficient cells. *TAGLN* transcripts were reduced in folate-deficient cells and increased in U0126-treated cells.

The detected gene expression changes are presumed to be a direct consequence of alterations in the folate pathway and associated metabolites, although it is possible that secondary effects of prolonged culture under low folate conditions lead to certain gene expression changes. If alterations in the folate pathway are directly involved, then it would be expected that treatment of the cells with methotrexate, a specific inhibitor of dihydrofolate reductase (see Fig. 1), should lead to similar gene expression changes. The fold changes in transcript levels of the same six genes were determined relative to untreated cells, using RNA isolated from human fibroblast cells treated with 1 μ M methotrexate for 24 h. The direction and degree of changes were similar between folate-deficient cells and the methotrexate cells for only *DKK1* and *WNT5A* (Fig. 5). However, no changes in transcript levels were observed for *FKSG42* and *EPHB6* (compared to a decrease in folate-deficient cells), and a slight decrease was detected in *WISP1*

(compared to an increase in folate-deficient cells). Values for *TAGLN* were more variable but slightly decreased as was detected in folate-deficient cells.

3.6. Response of the *DKK1* and *TAGLN* promoters to folate deficiency, methotrexate, homocysteine and U0126

The change in transcript levels due to folate deficiency can result from increases or decreases in promoter activity. To determine if promoter activity is affected by folate deficiency, we attempted to clone the gene promoters for a subset of the six selected genes. We were successful in cloning upstream regions of the *DKK1* and *TAGLN* genes into a luciferase reporter vector. Both gene transcripts were found to be decreased in folate-deficient cells (see Fig. 3). Stable lines of NIH3T3 cells, which contain these reporter constructs, were generated. The cells were grown in folate-sufficient and -deficient medium for 8 days, and equal numbers of cells were assayed for luciferase activity and total protein. Promoter activity decreased for both *DKK1* and *TAGLN* in folate-deficient cells relative to folate-sufficient cells (Fig. 6). These data suggest that the decrease in *DKK1* and *TAGLN* transcripts in folate-deficient cells is due to reduced transcription.

We also examined the response of the *DKK1* and *TAGLN* promoters to methotrexate, U0126 and homocysteine by treating the NIH3T3 stable cell lines containing the *DKK1* and *TAGLN* luciferase reporter constructs with these compounds. Methotrexate caused a decrease in the activity of both *DKK1* and *TAGLN* promoters (Fig. 7). The level of activity was reduced to approximately 23% for *DKK1* and 58% for *TAGLN*. These results correspond to those in Figs. 5 and 6, which show that both *DKK1* and *TAGLN* transcript levels and promoter activity are reduced in folate-

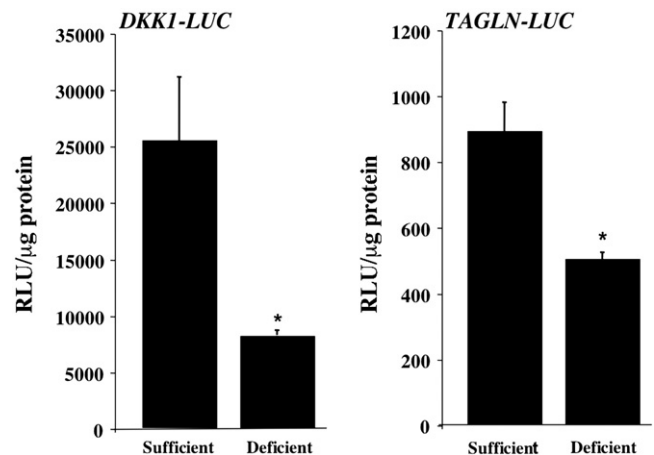


Fig. 6. *DKK1* and *TAGLN* promoter activity in NIH3T3 cells grown in folate-sufficient and -deficient medium. NIH3T3 cells that were stably transfected with *DKK1* and *TAGLN* luciferase reporter constructs (*DKK1*-LUC and *TAGLN*-LUC) were grown in folate-deficient and -sufficient medium for 8 days as described in Section 2. Equal numbers of cells were assayed for luciferase activity, and total protein was determined. Promoter activity is expressed as relative light units per microgram of protein. Error bars indicate \pm S.E.; $n=5$. *Significant difference ($P<.05$) as determined by the t test.

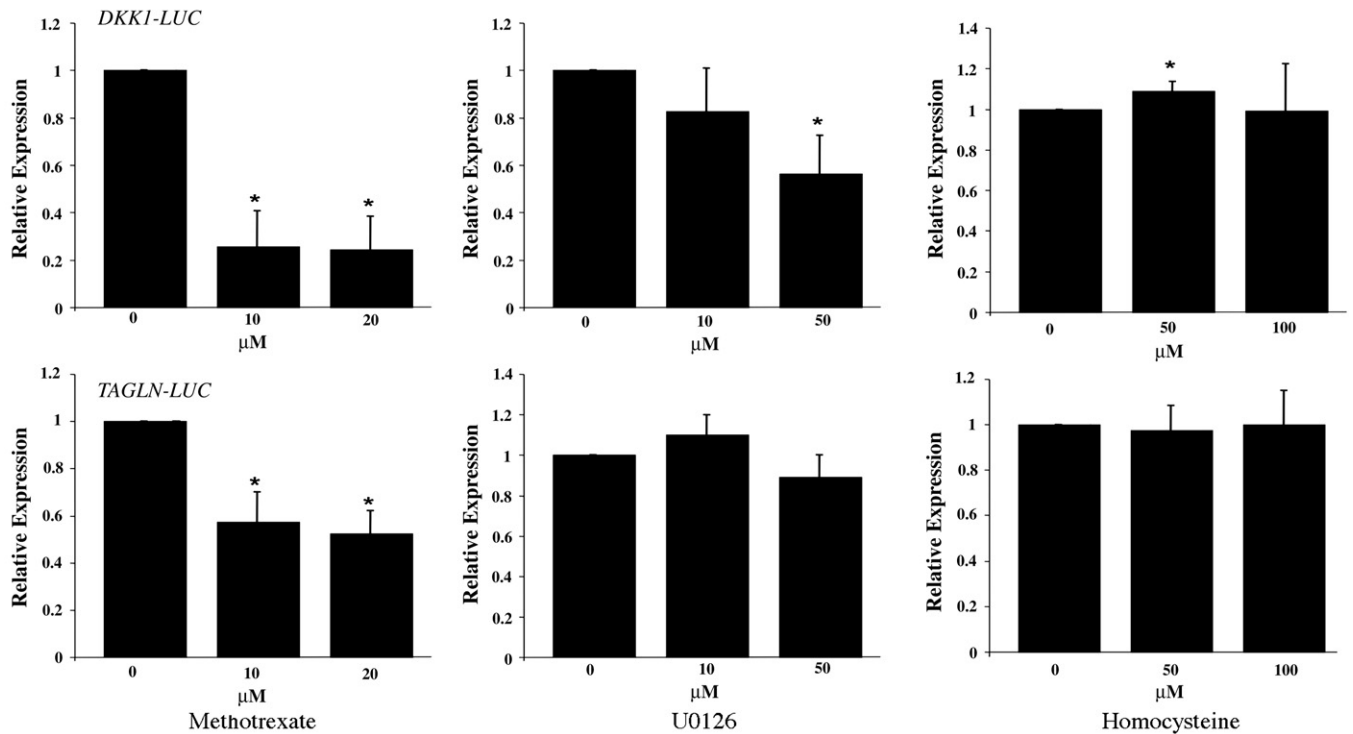


Fig. 7. *DKK1* and *TAGLN* promoter activity in NIH3T3 cells treated with methotrexate, U0126 and homocysteine. NIH3T3 cells that were stably transfected with *DKK1* and *TAGLN* luciferase reporter constructs were treated with the indicated concentrations for 24 h. Cellular lysates were assayed for luciferase activity, and total cellular protein was determined. The relative light units per microgram of protein for each sample were determined. These values were divided by the mean relative light units per microgram of protein of the control group for that treatment group to give a percent or relative expression. Error bars represent the calculated standard deviation of the percent value; $n=3$. *Significant difference ($P<.05$) as determined by the t test.

deficient cells. *DKK1* promoter activity was decreased at 50 μM U0126, whereas the *TAGLN* promoter was unaffected at either concentration. In comparison, *TAGLN* transcripts increased in U0126-treated cells and *DKK1* transcript levels decreased (see Fig. 5). This result suggests that the effect of U0126 on the *DKK1* transcript levels may, in part, be on the transcriptional level. Homocysteine had no effect on either gene promoter activity, a result consistent with the qRT-PCR data (Fig. 5).

4. Discussion

We have compared relative gene expression in normal human dermal fibroblast cells grown in folate-deficient medium for 7 days to cells grown in folate-sufficient medium via microarray analysis. Of the nearly 17,000 genes probed, 61 genes that displayed a relative change in transcript levels were selected based on the criteria of having the same direction of change on three out of four chips for both biological replicas and fold change values at the 95% confidence level for one replica or for both biological replicas. Significantly, relative gene expression changes for a subset of these genes were confirmed by qRT-PCR of multiple biological replicate samples (Figs. 3–5). What is most obvious when surveying the gene list is the lack of genes involved in DNA repair and checkpoint response and the predominance of genes with functions

related to cell signaling, extracellular matrix and cytoskeleton. Courtemanche et al. [32] found that genes involved in base and nucleotide excision repair, including uracil glycosylase and AOEX nuclease, were up-regulated in lymphocytes grown in folate-deficient medium for 10 days, whereas expression of genes associated with double strand breaks did not change. Two folate-metabolism-related genes were found to be up-regulated, whereas seven were found to be down-regulated. In our study, three genes associated with nucleotide metabolism were up-regulated, including thymidylate synthase, which converts dUMP to TMP (see Fig. 1), but genes associated with DNA damage and repair did not change. An obvious explanation for these differences is that folate deficiency has a greater effect on lymphocytes. Further comparisons are not possible as Courtemanche et al. used a chip with only 695 stress and aging genes.

Our results are more similar to those of Crott et al. [31]. In this study, young and old rats were depleted of folate for 20 weeks, and gene expression was compared in colonic mucosal cells using a 9000 gene microarray. Somewhat surprisingly, they found no overlap between the gene sets of folate-depleted, old and young rats, suggesting that the response of cells to folate deficiency is related to the developmental state of the cell. Our results that measure the expression of a subset of the fibroblast-selected genes in folate-deficient human lymphoblasts suggest that there are both conserved and cell-type-specific responses to folate

deficiency. It is likely, however, that folate deficiency causes gene changes unique to lymphoblasts that would not have been detected in our analysis. Direct comparison of the Crott et al. gene sets to ours yielded only one identical gene, *cathepsin C*, which is up-regulated in folate-depleted old rats. Other common but nonidentical gene sequences included *actin*, *matrix metalloproteinase* and *integrin*. However, known DNA damage and repair genes were absent from both gene sets.

Three of the genes focused on in this study code for secreted proteins associated with the Wnt pathway: *DKK1*, *WNT5A* and *WISP1*. The Wnt pathway has particular importance not only in developmental patterning but also in differentiation and replication of adult stem cell populations [41,42]. *DKK1* (dickkopf-1) is a 259 amino acid secreted protein that forms a complex with the Wnt receptors LRP5/6 and Kremen, inhibiting the activation of the Wnt pathway [43,44]. Induction of *DKK1* has been shown to involve the Wnt/ β -catenin signaling pathway [45,46]. *DKK1* expression was found to be down-regulated in colon tumors, indicating that *DKK1* is functioning as a tumor suppressor [45]. The link between folate deficiency and increased risk of colorectal cancer is presumed to be due primarily to increased genomic instability. Another possibility is that a reduction in *DKK1* expression may contribute to an environment more favorable to cancer formation, assuming that the *DKK1* protein levels are also decreased, by increasing the growth potential of the cell population. We also detected an increase in *WISP1* mRNA levels in folate-deficient cells, and *WISP1* mRNA was found to be overexpressed in colon tumors and cell lines [47], as well as in primary breast cancers [48,49]. In contrast, loss of *WNT5A* expression has been shown to lead to mammary epithelial cell transformation [50], whereas we found *WNT5A* to be up-regulated in folate-deficient cells.

Of particular relevance to our study is the finding that *DKK1* mRNA decreases and *WNT5A* mRNA increases in human adult bone marrow stem cells grown to stationary phase [41]. Similarly, we found a decrease in *DKK1* and an increase in *WNT5A* transcripts in folate-deficient cells. Moreover, *DKK1* transcript levels and promoter activity were decreased in cells treated with methotrexate and the Ras pathway inhibitor U0126. Together, these findings suggest that *DKK1* (and most likely *WNT5A*) expression is associated with growth of the cell population and/or the cell cycle. The folate-deficient, methotrexate- and U0126-treated cells were grown in medium containing serum and were maintained at subconfluent levels. Thus, the decrease in *DKK1* expression cannot be explained by the lack of growth factors or contact inhibition. One interpretation of our data is that *DKK1* expression requires the Ras pathway for expression and that folate deficiency is altering the Ras pathway. An alternative explanation is that the *DKK1* gene is responding to a decreased rate of DNA synthesis or growth rate (caused by folate deficiency, methotrexate or U0126) by some unknown pathway. In this case, *DKK1*

gene expression would be affected by folate deficiency primarily in dividing cell populations, such as in the embryo or stem cells. An indirect connection between *DKK1* and folate deficiency has been revealed in analyses of mutant mice displaying neural tube defects. The Crooked tail (*Cd*) cranial neural tube defect in mice, which is responsive to folate supplementation, was determined to result from a mutation in the LRP6 receptor. This mutation eliminated its *DKK1* binding site while maintaining its ability to activate the Wnt pathway [51]. Thus, in these *Cd* mice, Wnt signaling is not properly regulated by *DKK1*.

Methotrexate treatment of cells has been shown to decrease Ras protein methylation and Ras function [40]. In another study, gene expression in the anterior neural tube from knockout mouse embryos lacking the folate binding protein-1 (*Folbp*^{-/-}) was compared to the same mouse embryos whose mothers were supplemented with folic acid [52]. They found that the methyl transferase, *Icmt*, which was responsible for methylation of Ras and other CAAX proteins, along with other methyltransferases, was up-regulated in the folic-acid-supplemented embryos. Together, these findings support the notion that folate deficiency may impact the Ras pathway by altering Ras protein methylation. We found, with one exception, that the gene expression changes in cells treated with the MEK1/2 inhibitor U0126 are similar to those detected in folate cells. Transcripts of transgelin (*TAGLN*), which code for an actin cross-linking protein, were down-regulated in folate-deficient cells and up-regulated in U0126-treated cells (compare results in Figs. 3–5). This could be explained by the fact that transgelin gene regulation is complex and involves both Raf-dependent and -independent pathways [53]. Overall, these findings support the hypothesis that the Ras pathway may be altered in folate-deficient cells or, alternatively, genes regulated through the Ras pathway are more likely to be sensitive to folate deficiency. Moreover, these results suggest a link between the Ras, Wnt and folate pathways. It will be important to determine if Ras protein methylation and membrane association and the levels of activated MEK1/2 are altered in folate-deficient cells.

NIH3T3 cells stably transfected with *DKK1* and *TAGLN* luciferase reporter constructs were used to determine if the observed changes in transcript levels was also detected at the transcriptional level. Our results indicate that the decrease in *DKK1* and *TAGLN* transcripts in folate-deficient cells is due to reduced transcription, as promoter activity of both genes was found to decrease in folate-deficient cells. Methotrexate treatment of the *DKK1* and *TAGLN* reporter cell lines also leads to decreased promoter activity, indicating that the transcriptional effects may be directly linked to the folate pathway. It will be important to demonstrate that the promoter activity of genes showing increased transcript levels due to folate deficiency also increases in folate-deficient cells. We are currently cloning the promoter of the *WNT5A* gene for this purpose.

An additional explanation as to how folate deficiency may lead to altered gene expression is increased intracellular homocysteine due to a reduction in the folate pathway metabolite 5-methyl-THF (see Fig. 1). Our data do not support such a mechanism since homocysteine treatment of human fibroblast either had little effect on transcript levels or had an opposite effect compared to folate deficiency for the six assayed genes. In addition, neither the *DKK1* promoters nor the *TAGLN* promoters were sensitive to homocysteine. It is possible, however, that exogenously added homocysteine does not alter the intracellular SAH/SAM ratio in these cells or that another subset of the genes in Table 1 is sensitive to homocysteine levels.

Table 1 includes many additional genes that were impacted by folate deficiency but which were not analyzed in the same detail as the six selected genes in this study. The degree of change in transcript levels for these genes was relatively small and, on the average, less than twofold. However, the variety of these genes suggests that gene expression is broadly affected in folate-deficient cells and that these changes may influence cell growth and function. It will be critical to determine to what degree protein levels change for some of these genes and to assay for altered cell function based on the observed changes in transcript and protein levels.

In summary, a group of genes that respond to reduced folate conditions has been identified. The identities of these genes suggest an alternative mechanism as to how reduced folate is impacting cell function in addition to the known effects of folate deficiency on genomic stability. This mechanism involves effects on genes that function in or are linked to critical signaling pathways including Wnt and Ras. Even modest levels of folate deficiency would be expected to impact dividing cell populations by altering the expression of genes such as *DKK1* with the potential to alter the fate and function of a cell population. Currently, we are exploring, in more detail, the relationships between folate deficiency, *DKK1* gene expression and the Ras pathway.

Acknowledgments

This research was supported, in part, by the Intramural Research Program of NIH and NIEHS and by an internal grant from UNCG.

We would like to thank Kristina Flores and Cindy Innes of NIEHS for their expert suggestions. Krishn Sharma from UNCG is acknowledged for his assistance.

References

- [1] James SJ, Pogribna M, Pogribny IP, Melnyk S, Hine RJ, Gibson JB, et al. Abnormal folate metabolism and mutation in the methylenetetrahydrofolate reductase gene may be maternal risk factors for Down syndrome. *Am J Clin Nutr* 1999;70:495–501.
- [2] Pancharuniti N, Lewis CA, Sauberlich HE, Perkins LL, Go RC, Alvarez JO, et al. Plasma homocyst(e)ine, folate, and vitamin B-12 concentrations and risk for early-onset coronary artery disease. *Am J Clin Nutr* 1994;59:940–8.
- [3] Refsum H, Ueland PM, Nygard O, Vollset SE. Homocysteine and cardiovascular disease. *Annu Rev Med* 1998;49:31–62.
- [4] Welch GN, Loscalzo J. Homocysteine and atherothrombosis. *N Engl J Med* 1998;338:1042–50.
- [5] Snowdon DA, Tully CL, Smith CD, Riley KP, Markesbery WR. Serum folate and the severity of atrophy of the neocortex in Alzheimer disease: findings from the Nun study. *Am J Clin Nutr* 2000;71:993–8.
- [6] Kuhn W, Roebroek R, Blom H, van Oppenraaij D, Przuntek H, Kretschmer A, et al. Elevated plasma levels of homocysteine in Parkinson's disease. *Eur Neurol* 1998;40:225–7.
- [7] Kruman II, Kumaravel TS, Lohani A, Pedersen WA, Cutler RG, Kruman Y, et al. Folic acid deficiency and homocysteine impair DNA repair in hippocampal neurons and sensitize them to amyloid toxicity in experimental models of Alzheimer's disease. *J Neurosci* 2002;22:1752–62.
- [8] Kim YI. Folate and carcinogenesis: evidence, mechanisms, and implications. *J Nutr Biochem* 1999;10:66–88.
- [9] Choi SW, Mason JB. Folate and carcinogenesis: an integrated scheme. *J Nutr* 2000;130:129–32.
- [10] Smithells RW, Sheppard S, Schorah CJ. Vitamin deficiencies and neural tube defects. *Arch Dis Child* 1976;51:944–50.
- [11] Milunsky A, Jick H, Jick SS, Bruell CL, MacLaughlin DS, Rothman KJ, et al. Multivitamin/folic acid supplementation in early pregnancy reduces the prevalence of neural tube defects. *JAMA* 1989;262:2847–52.
- [12] Lucock MD, Daskalakis I, Lumb CH, Schorah CJ, Levene MI. Impaired regeneration of monoglutamyl tetrahydrofolate leads to cellular folate depletion in mothers affected by a spina bifida pregnancy. *Mol Genet Metab* 1998;65:18–30.
- [13] Shaw GM, Wasserman CR, Murray JC, Lammer EJ. Infant TGF- α genotype, orofacial clefts, and maternal periconceptional multivitamin use. *Cleft Palate Craniofac J* 1998;35:366–70.
- [14] Bienengraber V, Malek FA, Moritz KU, Fanghanel J, Gundlach KK, Weingartner J. Is it possible to prevent cleft palate by prenatal administration of folic acid? An experimental study. *Cleft Palate Craniofac J* 2001;38:393–8.
- [15] Kapusta L, Haagmans ML, Steegers EA, Cuypers MH, Blom HJ, Eskes TK. Congenital heart defects and maternal derangement of homocysteine metabolism. *J Pediatr* 1999;135:773–84.
- [16] Tang LS, Wlodarczyk BJ, Santillano DR, Miranda RC, Finnell RH. Developmental consequences of abnormal folate transport during murine heart morphogenesis. *Birth Defects Res A Clin Mol Teratol* 2004;70:449–58.
- [17] Choi SW, Kim YI, Weitzel JN, Mason JB. Folate depletion impairs DNA excision repair in the colon of the rat. *Gut* 1998;43:93–9.
- [18] Duthie SJ, Hawdon A. DNA instability strand breakage, uracil misincorporation, and defective repair is increased by folic acid depletion in human lymphocytes in vitro. *FASEB J* 1998;12:1491–7.
- [19] Duthie SJ, Grant G, Narayanan S. Increased uracil misincorporation in lymphocytes from folate-deficient rats. *Br J Cancer* 2000;83:1532–7.
- [20] Duthie SJ, Narayanan S, Blum S, Pirie L, Brand GM. Folate deficiency in vitro induces uracil misincorporation and DNA hypomethylation and inhibits DNA excision repair in immortalized normal human colon epithelial cells. *Nutr Cancer* 2000;37:245–51.
- [21] Jacob RA, Gretz DM, Taylor PC, James SJ, Pogribny IP, Miller BJ, et al. Moderate folate depletion increases plasma homocysteine and decreases lymphocyte DNA methylation in postmenopausal women. *J Nutr* 1998;128:1204–12.
- [22] Fowler BM, Giuliano AR, Piyathilake C, Nour M, Hatch K. Hypomethylation in cervical tissue: is there a correlation with folate status? *Cancer Epidemiol Biomarkers Prev* 1998;7:901–6.
- [23] Pufulete M, Al-Ghnam R, Leather AJ, Appleby P, Gout S, Terry C, et al. Folate status, genomic DNA hypomethylation, and risk of

- colorectal adenoma and cancer: a case control study. *Gastroenterology* 2003;124:1240–8.
- [24] Kim YI. Folate and DNA methylation: a mechanistic link between folate deficiency and colorectal cancer? *Cancer Epidemiol Biomarkers Prev* 2004;13:511–9.
- [25] Koury MJ, Horne DW, Brown ZA, Pietenpol JA, Blount BC, Ames BN, et al. Apoptosis of late-stage erythroblasts in megaloblastic anemia: association with DNA damage and macrocyte production. *Blood* 1997;89:4617–23.
- [26] Christman JK, Sheikhejad G, Dizik M, Abileah S, Wainfan E. Reversibility of changes in nucleic acid methylation and gene expression induced in rat liver by severe dietary methyl deficiency. *Carcinogenesis* 1993;14:551–7.
- [27] Pogribny IP, Miller BJ, James SJ. Alterations in hepatic p53 gene methylation patterns during tumor progression with folate/methyl deficiency in the rat. *Cancer Lett* 1997;115:31–8.
- [28] Pogribny IP, James SJ. De novo methylation of the p16INK4A gene in early preneoplastic liver and tumors induced by folate/methyl deficiency in rats. *Cancer Lett* 2002;187:69–75.
- [29] Fuso A, Seminara L, Cavallaro RA, D'Anselmi F, Scarpa S. S-adenosylmethionine/homocysteine cycle alterations modify DNA methylation status with consequent deregulation of PS1 and BACE and beta-amyloid production. *Mol Cell Neurosci* 2005;28:195–204.
- [30] Jhaveri MS, Wagner C, Trepel JB. Impact of extracellular folate levels on global gene expression. *Mol Pharmacol* 2001;60:1288–95.
- [31] Crott JW, Choi SW, Ordovas JM, Ditelberg JS, Mason JB. Effects of dietary folate and aging on gene expression in the colonic mucosa of rats: implications for carcinogenesis. *Carcinogenesis* 2004;25:69–76.
- [32] Courtemanche C, Huang AC, Elson-Schwab I, Kerry N, Ng BY, Ames BN. Folate deficiency and ionizing radiation cause DNA breaks in primary human lymphocytes: a comparison. *FASEB J* 2004;18:209–11.
- [33] Tang LS, Finnell RH. Neural and orofacial defects in *Folp1* knockout mice [corrected]. *Birth Defects Res A Clin Mol Teratol* 2003;67:209–18.
- [34] Kaufmann WK, Levedakou EN, Grady HL, Paules RS, Stein GH. Attenuation of G2 checkpoint function precedes human cell immortalization. *Cancer Res* 1995;55:7–11.
- [35] Heinloth AN, Shackelford RE, Innes CL, Bennett L, Li L, Amin RP, et al. ATM-dependent and -independent gene expression changes in response to oxidative stress, gamma irradiation, and UV irradiation. *Radiat Res* 2003;160:273–90.
- [36] Hamadeh HK, Bushel PR, Jayadev S, DiSorbo O, Bennett L, Li L, et al. Prediction of compound signature using high density gene expression profiling. *Toxicol Sci* 2002;67:232–40.
- [37] Chen Y, Dougherty E, Bittner M. Ratio-based decisions and the quantitative analysis of cDNA microarray images. *J Biomed Opt* 1997;2:364–74.
- [38] Horne DW, Patterson D. *Lactobacillus casei* microbiological assay of folic acid derivatives in 96-well microtiter plates. *Clin Chem* 1988;34:2357–9.
- [39] Wang X, Fenech M. A comparison of folic acid and 5-methyltetrahydrofolate for prevention of DNA damage and cell death in human lymphocytes in vitro. *Mutagenesis* 2003;18:81–6.
- [40] Winter-Vann AM, Kamen BA, Bergo MO, Young SG, Melnyk S, James SJ, et al. Targeting Ras signaling through inhibition of carboxyl methylation: an unexpected property of methotrexate. *Proc Natl Acad Sci U S A* 2003;100:6529–34.
- [41] Gregory CA, Singh H, Perry AS, Prockop DJ. The Wnt signaling inhibitor dickkopf-1 is required for reentry into the cell cycle of human adult stem cells from bone marrow. *J Biol Chem* 2003;278:28067–78.
- [42] Kuhnert K, Davis CR, Wang H-T, Chu P, Lee M, Yuan J, et al. Essential requirement for Wnt signaling in proliferation of adult small intestine and colon revealed by adenoviral expression of Dickkopf-1. *Proc Natl Acad Sci U S A* 2004;101:266–71.
- [43] Baffico A, Liu G, Yaniv A, Gazit A, Aaronson SA. Novel mechanism of Wnt signalling inhibition mediated by Dickkopf-1 interaction with LRP6/Arrow. *Nat Cell Biol* 2001;3:683–6.
- [44] Li L, Mao J, Sun L, Liu W, Wu D. Second cysteine-rich domain of Dickkopf-2 activates canonical Wnt signaling pathway via LRP-6 independently of dishevelled. *J Biol Chem* 2002;277:5977–81.
- [45] Gonzalez-Sancho JM, Aguilera O, Garcia JM, Pendas-Franco N, Pena C, Cal S, et al. The Wnt antagonist DICKKOPF-1 gene is a downstream target of beta-catenin/TCF and is downregulated in human colon cancer. *Oncogene* 2005;24:1098–103.
- [46] Chamorro MN, Schwartz DR, Vonica A, Brivanlou AH, Cho KR, Varmus HE. FGF-20 and DKK1 are transcriptional targets of beta-catenin and FGF-20 is implicated in cancer and development. *EMBO J* 2005;24:73–84.
- [47] Pennica D, Swanson TA, Welsh JW, Roy MA, Lawrence DA, Lee J, et al. WISP genes are members of the connective tissue growth factor family that are up-regulated in wnt-1-transformed cells and aberrantly expressed in human colon tumors. *Proc Natl Acad Sci U S A* 1998;95:14717–22.
- [48] Saxena N, Banerjee S, Sengupta K, Zoubine MN, Banerjee SK. Differential expression of WISP-1 and WISP-2 genes in normal and transformed human breast cell lines. *Mol Cell Biochem* 2001;228:99–104.
- [49] Xie D, Nakachi K, Wang H, Elashoff R, Koeffler HP. Elevated levels of connective tissue growth factor, WISP-1, and CYR61 in primary breast cancers associated with more advanced features. *Cancer Res* 2001;61:8917–23.
- [50] Olson DJ, Gibo DM. Antisense wnt-5a mimics wnt-1-mediated C57MG mammary epithelial cell transformation. *Exp Cell Res* 1998;241:134–41.
- [51] Carter M, Chen X, Slowinska B, Minnerath S, Glickstein S, Shi L, et al. Crooked tail (Cd) model of human folate-responsive neural tube defects is mutated in Wnt coreceptor lipoprotein receptor-related protein 6. *Proc Natl Acad Sci U S A* 2005;102:12843–8.
- [52] Spiegelstein O, Cabrera RM, Bozinov D, Wlodarczyk B, Finnell RH. Folate-regulated changes in gene expression in the anterior neural tube of folate binding protein-1 (*Folbp1*)-deficient murine embryos. *Neurochem Res* 2004;29:1105–12.
- [53] Shields JM, Rogers-Graham K, Der CJ. Loss of transgelin in breast and colon tumors and in RIE-1 cells by Ras deregulation of gene expression through Raf-independent pathways. *J Biol Chem* 2002;277:9790–9.